RESEARCH PAPER

Green synthesis, Physicochemical Characterization and LC-MS Based Phytochemical Profiling of *Tinospora cordifolia* stem mediated Gold Nanoparticles

Mounika kovvali[1], and Suseela Lanka*[1]

[1]Department of Biosciences and Biotechnology, Krishna University, Machilipatnam-521004, India.

***Corresponding Author:** suseela.bsbt@kru.ac.in, https://orcid.org/0000-0001-8843-8223

Abstract

A green and sustainable strategy was employed to synthesize aqueous gold nanoparticles using the medicinal plant *Tinospora cordifolia*. Phytochemical screening of the plant extract was performed to identify the secondary metabolites acting as reducing and stabilizing agents for the synthesis of gold nanoparticles from chloroauric acid. The formation of nanoparticles was evidenced by a distinct colour transition and a Surface Plasmon Resonance (SPR) peak at 535 nm, as observed via UV-Vis spectroscopy. Physicochemical characterization was further conducted using FTIR, SEM-EDX, TEM, XRD, DLS, and Zeta potential analysis. The combined results demonstrated that the synthesized gold nanoparticles were predominantly spherical, uniformly distributed, crystalline, and capped with functional groups derived from plant metabolites. LC-MS profiling identified four major phytoconstituents: Tinosporide,20-β-hydroxyecdysone, Jatrorrhizine, and Tetrahydropalmatine. The reduction of ionic gold was facilitated by these naturally occurring phytochemicals. Overall, the findings indicate that *Tinospora cordifolia* stem extract serves as an effective green source for producing stable, biocompatible gold nanoparticles with potential biomedical applications.

Keywords: *Tinospora cordifolia;* Plant Extract, green synthesis, Gold nanoparticles, Characterization, LC-MS, Phytoconstituents

How to cite this article: Kovvali M, Lanka S. Green Synthesis, Physicochemical Characterization and LC-MS Based Phytochemical Profiling of Tinospora cordifolia Stem Mediated Gold Nanoparticles. Int J Drug Deliv Technol. 2026;16(18s): 374-386. DOI: 10.25258/ijddt.16.18s.40.

Graphical Abstract:

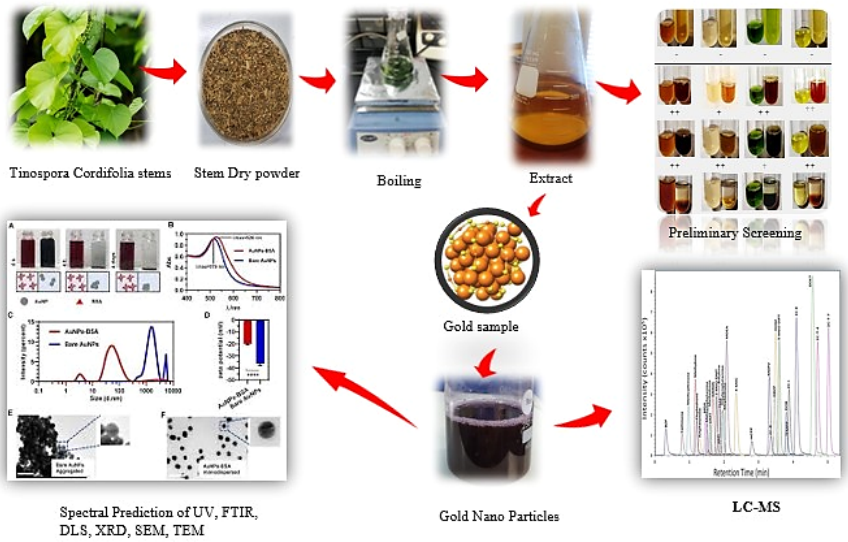

1. INTRODUCTION

Within traditional Indian medical practices, *Tinospora cordifolia* is regarded as a valuable therapeutic plant due to its diverse biological and pharmacological properties[1]. The stem of *Tinospora cordifolia* exhibits strong reducing and stabilizing capabilities, making it a suitable biological source for eco-friendly nanoparticle synthesis[2]. In green nanotechnology, plant-based extracts are preferred because they contain

*Author for Correspondence: suseela.bsbt@kru.ac.in

phytochemicals that can reduce metal ions into stable nanoparticles without the need for toxic chemicals[3,4]. In this study, the stem-derived extract of *Tinospora cordifolia* underwent a qualitative phytochemical assessment to elucidate the major groups of biologically active compounds[5]. These phytochemical constituents act as natural reducing agents, initiating the formation of gold nanoparticles (AuNPs) in the presence of metal precursors [6]. Following this preliminary evaluation, the extract was used to synthesize gold nanoparticles, which were systematically characterized using spectroscopic, microscopic, and diffraction techniques to investigate their optical behaviour, morphology, surface chemistry, crystallinity, and dispersion characteristics.

To identify the specific metabolites responsible for nanoparticle formation, an LC-MS-based analytical approach was employed[7]. This analysis revealed four major phytochemicals- 20-β-Hydroxyecdysone, Jatrorrhizine, Tetrahydropalmatine, and Tinosporide, each possessing functional groups capable of reducing and stabilizing the nanoparticles. The identification of these metabolites provides molecular-level insight into how *T. cordifolia* mediates synthesis[8]. Since these metabolites are known to exhibit antioxidant, anti-inflammatory, and cell-growth inhibitory effects, these gold nanoparticles are being widely investigated for drug delivery and targeted therapy[9][10]. Consequently, this work integrates plant chemistry, particle synthesis, and metabolite profiling to establish a foundation for exploring *T. cordifolia* stem-derived gold nanoparticles in biomedical and cancer-oriented research[11].

2. MATERIALS AND METHODS

2.1 Plant Source

Stem samples of *Tinospora Cordifolia*, collected from Machilipatnam, Andhra Pradesh, India, were verified for taxonomic identity by a qualified botanist at Acharya Nagarjuna University, Guntur. Gold nanoparticle synthesis was performed using $HAuCl_4.3H_2O_2$(hydrogen tetrachloroaurate (III) trihydrate, ≥99.8% Sigma-Aldrich) as the precursor salt, while deionised water served as the solvent in all experimental steps[3,12].

2.2 *Tinospora cordifolia* Stem Extract

The collected *Tinospora cordifolia* were cleaned thoroughly with running tap water to remove soil debris, then rinsed with deionised water to remove residual surface impurities. The cleaned stems were shade-dried under ambient conditions (approximately 28° C) for 10-12 days until fully dry. The dried stems were then chopped into small pieces and ground into a powder using a sterile mechanical grinder. 5% Aqueous extraction was prepared by heating at 70°C for 30 minutes with continuous magnetic stirring, then allowing it to cool to ambient temperature. It was passed through a Whatman No. 1 filter paper and subsequently centrifuged at 5000 rpm for 10 min to remove insoluble residues. The result was a clear extract, carefully collected and preserved at 4°C in sterile amber-coloured containers for further experimental use.

2.3 Preliminary Phytochemical Screening

The aqueous stem extract underwent qualitative phytochemical evaluation to identify by standard procedures were used to detect alkaloids (Wagner test), flavonoids (alkaline reagent test), phenols (iodine test), tannins (Gelatin test), saponins (foam test), glycosides (Borntrager test), terpenoids and steroids (Salkowski test), amino acids (ninhydrin test), and carbohydrates (Molisch's test). Observations were recorded and interpreted based on colour changes and precipitate formation[13].

2.4 Gold Nanoparticles (AuNPs) synthesis:

An aqueous solution of Cholo Auric Acid ($HAuCl_4$) at a concentration of 1mM was freshly prepared using deionised (DI) water. For nanoparticle synthesis, 50 mL of the *Tinospora cordifolia* stem extract was combined with 50 mL of the 1 mM $HAuCl_4$ solution in a 250 mL beaker, maintaining a 1:1 (v/v) ratio. The reaction mixture was continuously stirred at ambient temperature (approximately 28°C) to facilitate the reduction process. The reaction was allowed to proceed under ambient conditions for 2h to ensure complete conversion of Au^{3+} ions into elemental gold. Gold nanoparticles formed in the reaction mixture were separated by centrifugation at 10,000 rpm for 20 min. The collected nanoparticle pellet was washed three times with Deionised water to eliminate loosely bound phytochemical residues. Lastly, the purified gold nanoparticles were re-suspended in deionised water and stored at 4°C until further characterization[12,14].

2.5 Characterisation of Gold Nanoparticles

The synthesised *Tinospora cordifolia*-mediated gold nanoparticles were subsequently treated with a series of physicochemical characterisation techniques to confirm their formation, structural properties, surface chemistry, and stability.

2.5.1 Ultra Violet - Visible Spectroscopy

The progression of gold ion reduction and nanoparticle formation was evaluated using UV–Visible spectroscopy. Absorption spectra of the colloidal gold nanoparticle solution were measured across the wavelength range of 200–800 nm using quartz cuvettes, with deionised water as the reference.

2.5.2 DLS and Zeta Potential Analysis

The hydrodynamic particle size distribution, polydispersity index, and surface charge characteristics of the biosynthesised gold nanoparticles were evaluated using a Zetasizer Nano ZS (Malvern Instruments), which operates on the principles of Dynamic Light Scattering and Electrophoretic Light Scattering.

For DLS measurements, the gold nanoparticle suspension was diluted 10-fold with double-distilled water to reduce interparticle interactions and minimise multiple-scattering effects. The measurements were carried out at 25 °C with a fixed backscattering angle of 173. The mean hydrodynamic diameter and PDI values were determined based on the mean of three independent measurements.

Zeta potential analysis was carried out using the same diluted nanoparticle suspension loaded into a disposable folded capillary cell (DTS1070). The electrophoretic mobility of the nanoparticles was determined by laser Doppler velocimetry, and the corresponding zeta potential values were automatically computed using the Smoluchowski model. All experiments were carried out in triplicate to ensure reliable and reproducible results.

2.5.3 Fourier Transform Infrared Spectroscopy

FTIR analysis was carried out to characterize the chemical functionalities associated with the nanoparticles, to examine the functional groups of plant stem-derived phytochemicals participating in the reduction process of Au^{3+} ions and the surface stabilisation preventing aggregation of the synthesised gold nanoparticles[15,16]. The AuNP samples were first lyophilised, then thoroughly mixed with dry potassium bromide to form homogeneous pellets. Infrared spectrum recorded over a spectral window of 4000–400 cm^{-1} using a resolution of 4 cm^{-1} to detect vibrational bands corresponding to functional groups associated with phytochemical capping of the gold nanoparticles.

2.5.4. X-ray Diffraction

XRD was performed to investigate the crystalline characteristics of the synthesised gold nanoparticles using a Rigaku Mini Flex 600 diffractometer with Cu Kα radiation (λ = 1.5406 Å). Diffraction patterns collected over a 2θ range of 10°–80° at a scan speed of 2° min^{-1}. The observed diffraction peaks were indexed, matched with standard reference data from the JCPDS database (Card No. 04-0784) to verify the formation of face-centred cubic (fcc) gold[17].

2.5.5 TEM (Transmission Electron Microscopy)

TEM was conducted to examine the particle size, morphology and crystalline features of the synthesized gold nanoparticles. One aliquot of the colloidal nanoparticle dispersion was carefully mounted on a carbon-coated copper grid and dried naturally under laboratory conditions before analysis. Then, imaging was performed at an accelerating voltage of 200 kV. The acquired Transmission electron microscopy micrographs enabled direct assessment of nanoparticle shape and size distribution, revealing predominantly spherical particles, and the crystalline nature of the gold nanoparticles was verified using selected area electron diffraction patterns.

2.5.6. SEM and Energy Dispersive X-ray Analysis

The morphology of the synthesised gold nanoparticles was examined using scanning electron microscopy, in which dried samples were secured and mounted on aluminium stubs using conductive carbon tape, sputter-coated to improve conductivity, and analysed under high-vacuum conditions at different magnifications [6]. Elemental composition was analysed using scanning electron microscopy coupled with energy-dispersive X-ray spectroscopy to verify the presence of gold and exclude impurities. A strong characteristic peak around 2.2 keV in the EDX spectrum was used to confirm the presence of elemental gold.

2.6. LC–MS Analysis

Metabolite analysis was conducted using an Agilent Ultivo Triple Quadrupole LC–MS platform. Before analysis, the biosynthesised gold nanoparticle of the *Tinospora cordifolia* stem solution was centrifuged, and the clear supernatant containing the phytochemical-bound gold nanoparticle fraction was injected into the LC column to identify the metabolites involved in nanoparticle formation.

Chromatographic separation of metabolites was carried out on a C18 reversed-phase column (2.1 × 100 mm, 1.8 µm) maintained at 40°C. The mobile phase system comprised water containing 0.1% formic acid (Solvent A) and acetonitrile supplemented with 0.1% formic acid (Solvent B). Metabolite elution was achieved using a linear gradient program ranging from 5% to 95% Solvent B over 20 min, with a constant flow rate of 0.3 mL min^{-1}. Mass spectra were acquired in positive electrospray ionisation (ESI^+) mode, with data acquisition carried out over an m/z range of 100-1000. Instrumental source conditions, including temperature, gas, nebuliser pressure, and capillary voltage, were optimised to ensure stable ionisation and sensitive detection of analytes. Compound identification was carried out by comparing exact mass, isotope distribution, and fragmentation spectra, mass by mass, with spectral databases, including PubChem, MassBank, NIST, and the Agilent built-in library. Structural predictions of matched metabolites were automatically generated and manually verified with published literature on *Tinospora cordifolia* phytochemicals[18,19].

This approach enabled the identification of key metabolites in the gold nanoparticle-containing solution, confirming which compounds actively mediated gold-ion reduction and subsequent nanoparticle stabilisation.

3. RESULTS AND DISCUSSION

3.1 Stem Extract

The clear aqueous extract obtained from the stem yielded a brownish filtrate, indicating efficient solubilisation of phytochemicals Figure 1. The extraction conditions were optimised to prevent heat-sensitive bioactive compounds from being lost later, which contributed to the median of gold reduction

followed by the nanoparticle stabilization, as confirmed by subsequent phytochemical screening and gold nanoparticle preparation[20].

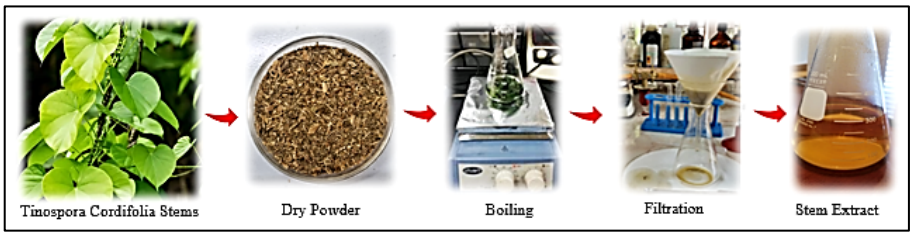

Figure. 1: Preparation of *Tinospora cordifolia* stem extract

3.2 Qualitative Phytochemical Screening

Initial phytochemical evaluation of the *Tinospora cordifolia* aqueous stem extract revealed diverse classes of secondary metabolites that are widely reported to facilitate the biosynthesis of gold nanoparticles. A summary of the results was provided in Table 1. The high abundance of alkaloids and steroids indicated that the extract contains strong capping and reducing agents. These phytochemicals possess functional groups such as O-H (phenols), C=O (alkaloids and proteins), C-N (alkaloids), and C-O-C (terpenoids and steroids). These were known to reduce Au^{3+} to Au^{0} and stabilize gold nanoparticles by surface adsorption. Phytoconstituents such as Saponins, Flavonoids, and Carbohydrates contribute to colloidal stabilisation through steric or electrostatic interactions. This phytochemical richness of *Tinospora cordifolia* confirms why the extract successfully mediates efficient gold nanoparticle synthesis[21].

S.NO	Phytochemical Constituents	Test Performed	Observation	Inference	Reference
1	**Alkaloids**	**Wagner's Test:** 1 mL of the filtrate with Wagner's reagent, resulting in a reddish-brown precipitate interface indicating the presence of alkaloids.		High Presence	[22]
2	**Flavonoids**	**Alkaline reagent Test:** 1 mL of the sample with 2 mL of 2% NaOH solution, develops a yellow colour, which disappears upon the addition of dilute HCl, thereby confirming the presence of flavonoids		Moderate presence	[23]
3	**Phenolic compounds**	**Iodine Test:** Treatment of 1 mL of the extract with a few drops of dilute iodine solution produced a transient red colouration, indicating the presence of phenolic compounds.		High Presence	[24]
4	**Tannins**	**Gelatin Test:** 1 mL of the extract, 1% Gelatin and 10% NaCl, leading to the formation of a white precipitate.		High Presence	[22]
5	**Saponins**	**Foam Test:** Vigorous shaking of 0.5 g of the extract with 2 mL of water produced foam, which disappeared after 10 minutes**.**		Moderate Presence	[25]

6	**Glycosides**	**Borntrager's test:** 2 mL of the hydrolysed filtrate is mixed with 3 mL of chloroform and shaken thoroughly. After phase separation, the chloroform layer was treated with 10% ammonia solution, producing a pink colouration indicative of glycosides.		Traces	[26]
7	**Terpenoids**	**Salkowski test:** 1mL of the extract was mixed with chloroform, filtered, and then treated with a few drops of concentrated sulfuric acid; the appearance of a golden yellow layer at the bottom confirmed the presence of triterpenoids		High Presence	[26,27]
8	**Steroids**	**Salkowski test:** 1 mL of the extract was mixed with chloroform, filtered, and subsequently treated with concentrated sulfuric acid; the appearance of a red-coloured lower layer indicated the presence of steroids		High Presence	[27]
9	**Proteins and amino acids**	**Ninhydrin test:** 2mL of the filtrate was treated with two drops of ninhydrin solution, resulting in the development of a violet colour, indicating the presence of proteins and amino acids.		Moderate Presence	[28]
10	**Carbohydrates**	**Molisch's test:** 1 mL of the aqueous extract was treated with alcoholic α-naphthol, followed by the careful addition of concentrated sulfuric acid along the sides of the test tube; the formation of a violet ring at the interface confirmed the presence of carbohydrates.		Moderate Presence	[29]

Table 1. Phytochemical Analysis of *Tinospora cordifolia* Stem Extracts

3.3 Visual Observation of gold nanoparticles

The generation of gold nanoparticles using the aqueous stem extract of *Tinospora cordifolia* was first confirmed by visual inspection of the reaction mixture. When the stem extract is combined with a 1 mM $HAuCl_4$ solution in a (v/v) ratio, a rapid transition in colour from pale yellow to ruby was observed within approximately 10 min, as shown in Figure 2. This colour has changed with well recognized optical signature of gold nanoparticle generation and is associated with the surface plasmon resonance phenomenon[30]. The developed ruby-red colour indicates the effective reduction of Au^{3+} ions to elemental gold (Au^0), mediated by bioactive phytochemicals present in the *Tinospora cordifolia* stem extract.

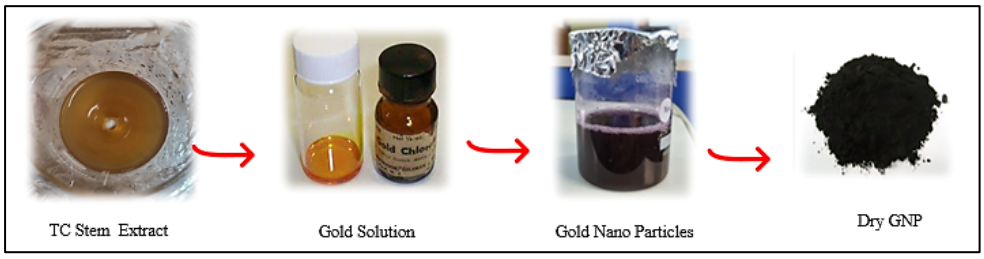

Figure 2: Green Synthesis of gold nanoparticles using *Tinospora cordifolia* stem extract

3.4 Characterisation of gold nanoparticles

3.4.1 UV-Visible spectroscopic Analysis

The formation of gold nanoparticles utilising the aqueous stem extract of Tinospora cordifolia was further verified by UV-Visible spectroscopic analysis Figure 3. The recorded UV-Visible spectrum displayed a prominent absorption maximum at 535nm, characteristic of the surface plasmon resonance of nanoscale gold nanoparticles. The occurrence of a surface plasmon resonance absorption band at 535nm confirmed the effective conversion of Au^{3+} ions into elemental gold Au^{0} facilitated by phytochemical constituents presented in the *Tinospora cordifolia* stem Extract[15]. The location of this absorption maximum indicates the formation of predominantly spherical gold nanoparticles in the nanoscale range, consistent with previously reported plant-mediated gold nanoparticle systems [12,31,32].

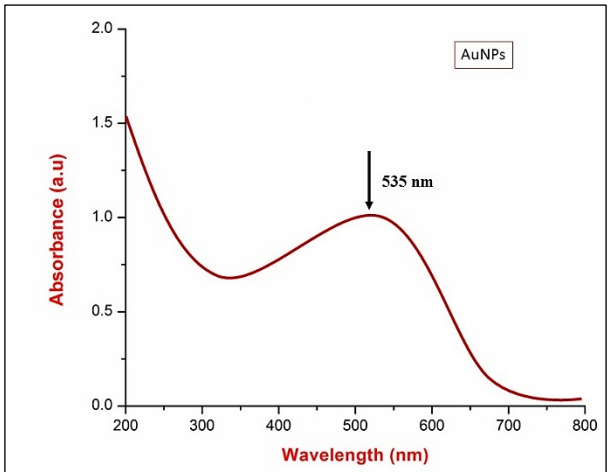

Figure 3. UV Visible spectrum of *Tinospora cordifolia* mediated gold nanoparticles showing a prominent surface plasmon resonance peak at 535 nm, indicative of nanoparticle formation.

3.4.2. Dynamic light scattering and zeta analysis

Dynamic light scattering and zeta potential measurements were carried out to analyse the hydrodynamic particle size distribution and surface charge behaviour of gold nanoparticles synthesised using *Tinospora cordifolia* stem extract, Figure 4(a). Dynamic light scattering analysis showed that the *Tinospora cordifolia* mediated gold nanoparticles possessed a narrow and unimodal hydrodynamic size distribution, with most particles distributed in the range of ~30–60 nm and an average size around ~40 nm. The absence of multiple peaks indicates that the nanoparticles were well-dispersed and monodisperse. The slightly larger size observed by dynamic light scattering compared to microscopic techniques can be attributed to the hydration layer and phytochemical capping molecules present on the nanoparticle surface[10].

Zeta potential measurements revealed a single dominant peak at 5-10 mV, indicating a moderately negative surface charge, as shown in Figure 4(b). This negative potential arises from the adsorption of plant-derived phytochemicals, including alkaloids, diterpenoids and steroidal compounds at the interface of the gold nanoparticle surface[15]. Although the absolute zeta potential value is moderate, and such behaviour is typical for green synthesising nanoparticles, where steric stabilisation by biomolecules plays a major role alongside electrostatic interactions[33].

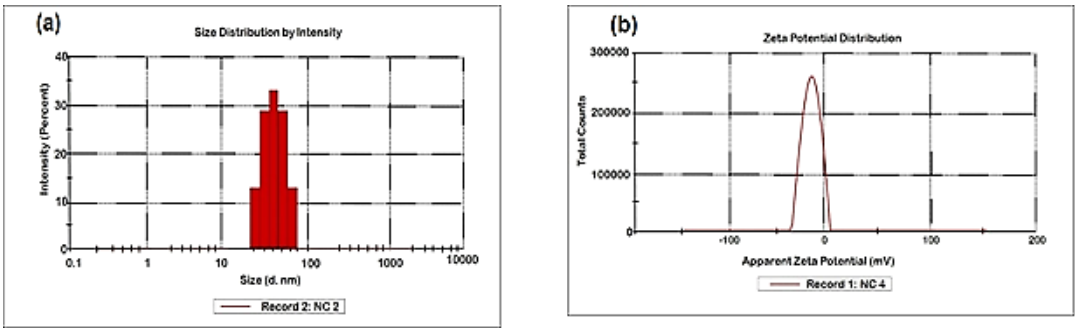

Figure 4. (a)DLS size distribution and (b) zeta potential profile of *Tinospora cordifolia stem–mediated* gold nanoparticles showing monodisperse particle size and moderate negative surface charge.

3.4.3. Fourier Transform Infrared spectroscopy Analysis

Fourier Transform Infrared Spectroscopy was employed to examine the functional groups associated with gold ion reduction and subsequent nanoparticle stabilisation of *Tinospora cordifolia* mediated gold nanoparticles, as shown in Figure 5. The FTIR spectrum exhibited several characteristic absorption bands corresponding to bioactive phytochemicals adsorbed on the AuNP surface.

A broad absorption feature detected around 3272 cm^{-1} is assigned to O–H stretching vibrations, indicating the presence of hydroxyl-bearing phytochemicals such as phenols, flavonoids, and steroidal constituents[34]. These hydroxyl functionalities are known to facilitate the reduction of Au^{3+} ions and help prevent aggregation of the resulting gold nanoparticles via surface

interactions. The absorption bands were observed at 2922 cm^{-1} and 2851 cm^{-1}, corresponding to aliphatic C-H stretching vibrations, indicating the contribution of terpenoid and alkaloid-related molecular frameworks present in the *Tinospora cordifolia* stem extract. The absorption band at 1625 to 1543 cm^{-1} corresponds to C=O stretching and N-H bending vibrations, indicating the involvement of alkaloids and proteinaceous components in the nanoparticle capping. The other additional peaks at 1375 to 1405 cm^{-1} are associated with C-N stretching and O-H bending, further supporting the presence of nitrogen-containing alkaloids such as Jatrorrhizine and Tetrahydro palmatine identified by LC-MS. And additional bands observed in the region 1237 to 1021 cm^{-1} correspond to C-O and C-O-C stretching vibrations, characteristic of Diterpenoids and steroidal compounds such as Tinosporide and 20-β-hydroxy ecdysone [16]. This analysis demonstrates that multiple functional groups in *Tinospora Cordifolia* metabolites contribute to gold-ion reduction and nanoparticle surface capping. The findings correlate well with LC-MS metabolite profiling and support the formation of stable, phytochemical-coated Gold Nano Particles[35].

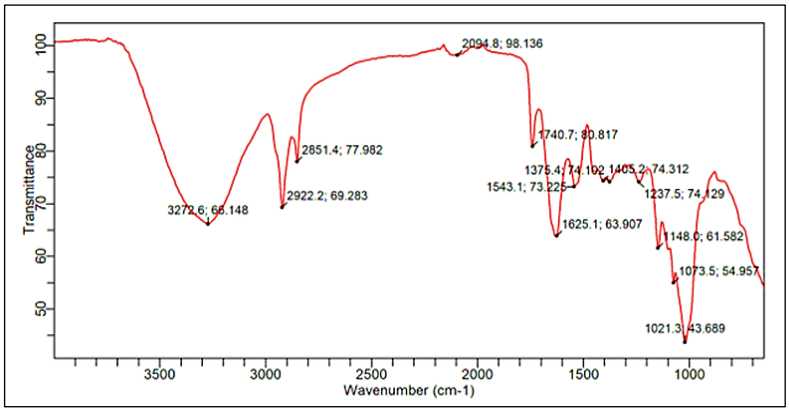

Figure 5. FTIR spectrum of *Tinospora cordifolia* mediated gold nanoparticles showing functional groups associated with phytochemical reduction and stabilization.

3.4.4. X-Ray Diffraction Analysis

The crystalline features and phase identity of *Tinospora cordifolia* mediated gold nanoparticles were evaluated through X-ray diffraction analysis Figure 6. which revealed well-defined diffraction peaks indicative of a crystalline structure. Distinct diffraction peaks were detected at 20 positions of 31.90°, 33.37°, 35.84°, 41.08°, 45.62°, 49.68°, 54.33°, 62.63°, 64.18°, and 75.46°. The observed reflections corresponded to the lattice planes of the face-centred cubic structure of gold, indicating successful crystallisation of elemental Au_4. Among these peaks, the intense peaks observed at ~31.9°, ~35.8°, and ~45.6° indicate high crystallinity, while the presence of multiple reflections confirms the polycrystalline nature of the gold nanoparticles. The relatively sharp peaks indicate good crystalline formation, whereas minor peak expansion suggests nanoscale particle size[36]. The absence of additional impurity peaks related to gold and other crystalline by-products confirms the high purity of the biosynthesised gold nanoparticles. Minor background noise observed in the diffractogram could be attributed to amorphous phytochemical capping layers derived from *Tinospora cordifolia* metabolites coating the gold nanoparticle surface[37].

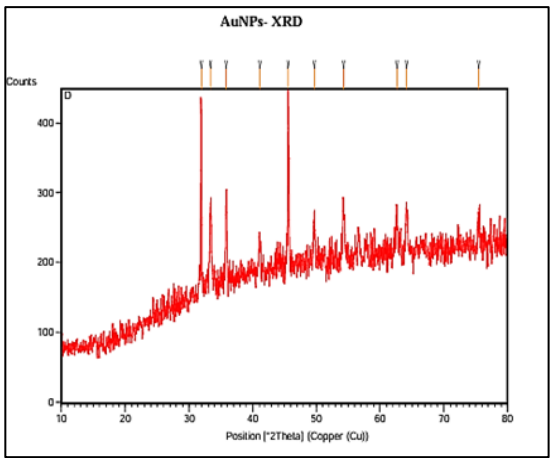

Figure 6. X-ray Diffraction pattern of *Tinospora cordifolia* stem-mediated gold nanoparticles confirming their crystalline, face-centred cubic structure.

3.4.5. Scanning Electron Microscopy and Energy Dispersive X- Ray

Surface morphology of *Tinospora cordifolia* stem mediated gold nanoparticles was examined through scanning electron microscopy, as shown in Figure 7(a),(b),(c). The micrograph revealed well-formed nanoparticle aggregates embedded in an organic matrix. The bright contrast observed in the image corresponded to gold nanoparticles, while the surrounding matrix was attributed to plant-derived photochemical capping layers. The observed aggregation is typical of green-synthesised nanoparticles, in which bioactive compounds act as stabilising agents and remain adsorbed on the nanoparticle surface. The morphology suggests effective nucleation and growth of gold nanoparticles within the phytochemical-rich environment provided by the *Tinospora cordifolia* stem extract[30,38].

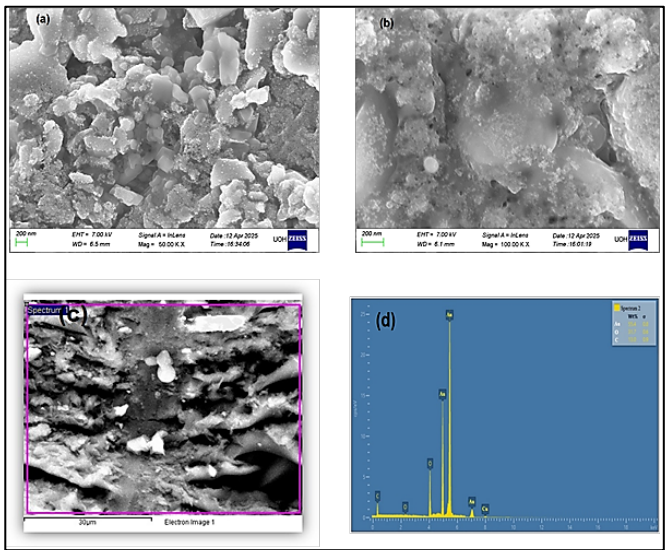

Figure 7. Scanning electron microscopy micrograph showing the surface morphology of *Tinospora cordifolia* stem mediated gold nanoparticles (a),(b),(c) and corresponding Energy Diffraction X-ray spectrum confirming the presence of elemental gold (d)

Elemental composition of the biosynthesised gold nanoparticles was confirmed through Energy Dispersive X-ray analysis, as illustrated in Figure 7 (d). The EDX spectrum showed a strong and characteristic signal for gold (Au) with prominent peaks around 2.2 keV and 9–10 keV, confirming the formation of elemental gold nanoparticles[32]. In addition to gold, weak signals attributable to carbon (C) and oxygen (O) were also observed. These elements originate from the organic phytochemicals bound to the nanoparticle surface, further supporting the role of plant metabolites as natural capping agents. The presence of a weak copper (Cu) signal can be attributed to the copper sample holder or grid used during SEM–EDX analysis and does not indicate contamination of the synthesised nanoparticles[39].

3.4.6. Transmission Electron Microscopy Analysis

TEM observations revealed that the biosynthesised gold nanoparticles exhibited a largely spherical morphology with particle diameters of approximately 10 nm, 100 nm, and 500 nm, as evidenced by the 10 nm scale bar shown in Figure 8. The nanoparticles appeared dark and electron-dense, confirming the formation of metallic gold cores. A relatively narrow size distribution was observed, which indicates controlled nucleation and growth during biosynthesis[27].The particle size obtained from the transmission electron microscope was smaller than the hydrodynamic diameter measured by dynamic light scattering. This was expected, since transmission electron microscopy measures the actual core size, whereas dynamic light scattering reflects the hydrated, phytochemical-capped size of the gold nanoparticles in solution. The Selected Area Electron Diffraction (SAED) showed clear concentric diffraction rings, confirming the polycrystalline character of the synthesised gold nanoparticles and also supporting the face-centred cubic structure observed in the X-ray diffraction results[40,41].

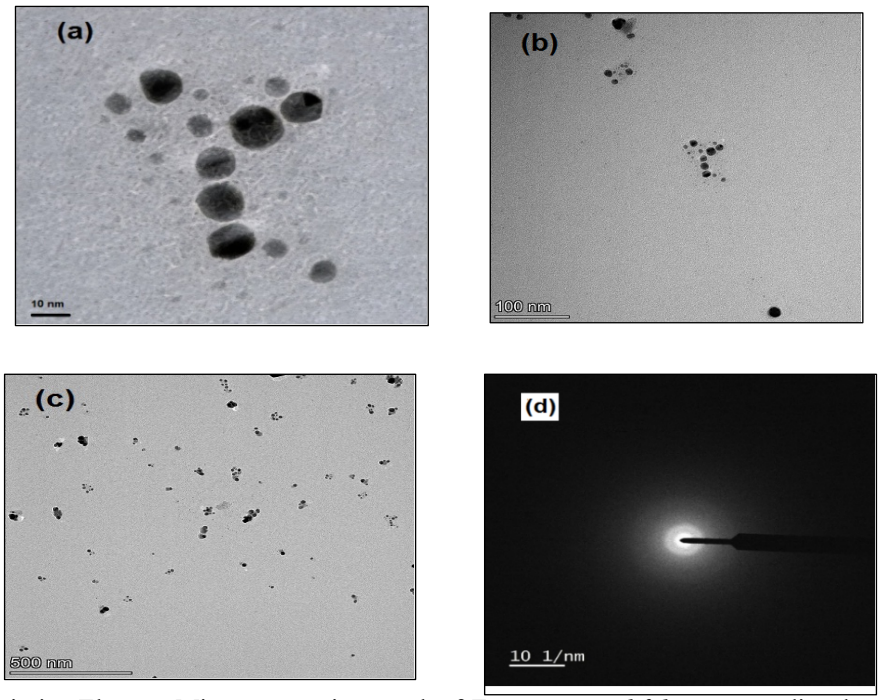

Figure 8. Transmission Electron Microscopy micrograph of *Tinospora cordifolia* stem mediated gold nanoparticles showing spherical particles with sizes in the range of 10 nm at a 10 nm scale, along with the corresponding SAED pattern confirming their polycrystalline nature.

3.5. LC – MS Metabolite Profiling

LC-MS analysis of the *Tinospora cordifolia* stem-mediated gold nanoparticle solution showed four main phytochemical components. Each one had a unique molecular ion peak and retention time, as shown in Figure 9. These metabolites fall into important bioactive groups like diterpenoid lactones, Ecdysteroids, and Isoquinoline/aporphine alkaloids. Identifying these compounds in the gold nanoparticle dispersion suggests they play a direct role in reducing gold ions and stabilising nanoparticles through surface interactions[19].

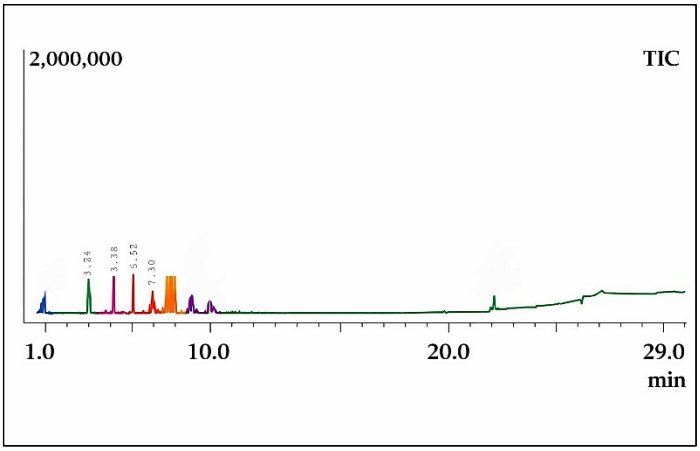

Figure 9. Total Ion Chromatogram (TIC) of the gold nanoparticle-containing solution showing major eluted phytochemical peaks.

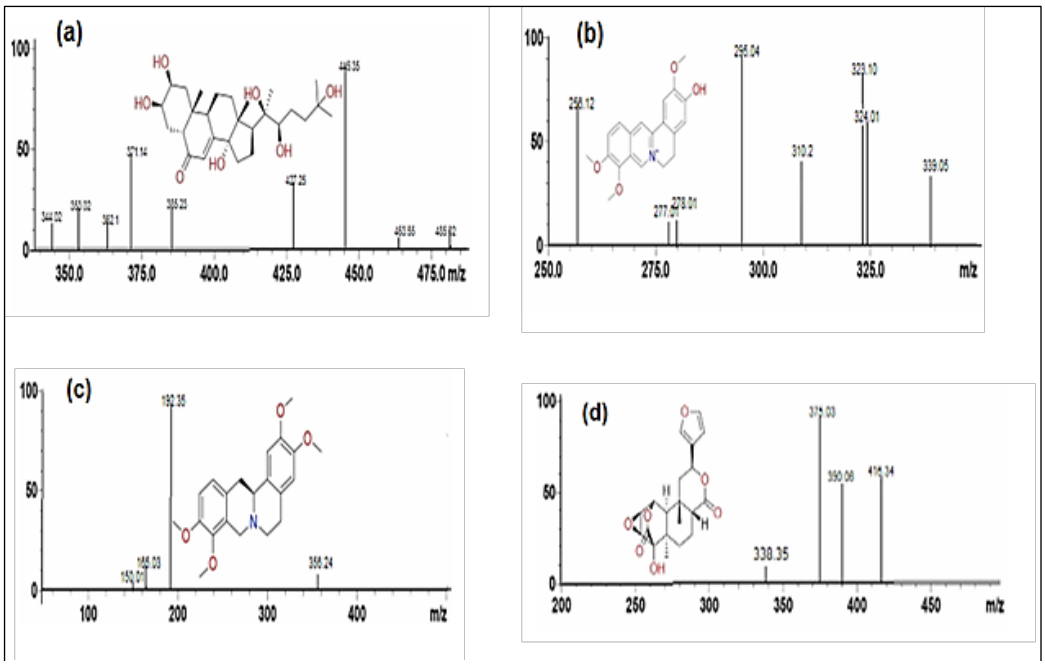

Figure 10. (a–d) Representative MS/MS spectra and proposed chemical structures of the identified bioactive metabolites:(a) 20-β-Hydroxy ecdysone, (b) Jatrorrhizine, (c) Tetrahydropalmatine and (d) Tinosporide.

Tinosporide, 20-β-hydroxyecdysone, Jatrorrhizine, and Tetrahydropalmatine were represented by four prominent peaks on the LC-MS chromatogram. Alkaloids, terpenoids, and steroidal compounds are confirmed to be present in the extract and to actively participate in the biosynthesis of gold nanoparticles by these metabolites, matching the major phytochemical classes found during preliminary screening[7,42].

Detected at m/z 481 (Rt 3.24 min), 20-β-Hydroxyecdysone has several hydroxyl groups that easily interact with metal ions, which explains how it contributes to the uniform size distribution and stabilisation of nanoparticles, as in Figure 10 (a). Jatrorrhizine showed a protonated molecular ion at m/z 339, with a retention time of 3.38 minutes. Isoquinoline alkaloids are known for their strong electron-donating properties. These properties aid in the reduction of metal ions, as in Figure 10 (b)[31]. Tetrahydropalmatine has a mass-to-charge ratio of 356 and a retention time of 5.52 minutes. It has structural features that make it suitable for binding metals and coating surfaces. This ensures that the nanoparticles remain stable over the long term. Figure 10 (c). A strong molecular ion peak at m/z ~416 was detected for Tinosporide with a retention time of 7.30 min. This finding matches its diterpenoid lactone structure, Figure 10 (d) [43]. Its abundant hydroxyl and lactone groups give it reducing power, which explains its key role in converting Au^{3} to Au^{2+}.

Together, these four compounds form a metabolite system that enhances the reduction, nucleation, and stabilisation of gold nanoparticles Table 2. Their known antioxidant, anti-inflammatory, and cytotoxic properties also show how *T. cordifolia*-derived AuNPs could be important for future cancer treatments. Phytochemical-coated nanoparticles may improve therapeutic performance [44,45].

Table 2: LC-MS derived metabolite compounds and their biological usage.

S. No	Compound Name	Molecular Formula	Retention Time (min)	Chemical Nature	Biological / Pharmacological Usage	Reference
1	**20-β-Hydroxy ecdysone**	$C_{27}H_{44}O_7$	3.24	Ecdysteroid	Known for anabolic, adaptogenic, antioxidant and cell-protective properties; enhances nanoparticle stability through multiple hydroxyl groups	[18]
2	**Jatrorrhizine**	$C_{20}H_{20}NO_4^+$	3.38	Isoquinoline alkaloid	Exhibits strong antimicrobial, antioxidant, anticancer and redox-active properties; promotes reduction of metal ions	[46]
3	**Tetrahydropalmatine**	$C_{21}H_{25}NO_4$	5.52	Aporphine alkaloid	Has analgesic, neuroprotective, and antioxidant activities; participates in	[47]

					metal chelation and nanoparticle stabilisation	
4	**Tinosporide**	$C_{20}H_{22}O_7$	7.30	Diterpenoid lactone	Exhibits antioxidant, anti-inflammatory, immunomodulatory and cytoprotective activities; contributes to metal ion reduction and stabilisation in nanoparticle synthesis.	[43]

4. CONCLUSION

The present study demonstrates that phytochemicals in the *Tinospora cordifolia* stem extract directly participate in the green synthesis of gold nanoparticles (AuNPs). Preliminary phytochemical screening confirmed the presence of diverse metabolite classes, while LC-MS analysis identified specific bioactive compounds, including Tinosporide, 20-β-hydroxyecdysone, Jatrorrhizine, and Tetrahydropalmatine, as key molecules driving nanoparticle formation. These metabolites functioned as natural reducing and capping agents, facilitating the production of stable, crystalline gold nanoparticles with precise nanoscale dimensions. TEM analysis revealed that the synthesized AuNPs were predominantly spherical, with diameters ranging from 10 to 30 nm, indicating excellent morphological control during biosynthesis. The favourable physical and chemical features of the gold nanoparticles, such as their controlled size, crystallinity, and phytochemical surface treatment, demonstrate the effectiveness of *Tinospora cordifolia* stem-mediated green synthesis. Given the known biological importance of the identified metabolites and the clear nanoscale properties of the synthesised gold nanoparticles, the phytochemical-coated gold nanoparticles could serve as a promising platform for future biological and cancer-related studies.

Conflict of Interest

Both authors have no conflicts of interest, financial or otherwise, that could have appeared to influence the work reported in this paper.

Declaration on Research Involving Human Participants and/or Animals

This article does not contain any studies with human participants or animals performed by any of the authors, and no funding from any other government or private agencies was obtained for this project

Author contributions

The authors have made their contributions towards the preparation of the manuscript. The details of the same are as follows: **Mounika kovvali**: Formal draft, material synthesis, and experimental work; Manuscript drafting. **Suseela Lanka**: Conceptualisation, Methodology, Analysis & Finalization and Editing of manuscript. Both authors read and approved the final manuscript.

Authors' ORCIDs:
Mounika Kovvali, mounika.karuna@gmail.com, https://orcid.org/0009-0004-0771-8362
Suseela Lanka , suseela.bsbt@kru.ac.in,https://orcid.org/0000-0001-8843-8223

REFERENCES

1. Saha, Soham; Ghosh, Shyamasree., Ancient Science of Life, 2012 vol. 31(4), p. 151-159. https://doi.org/10.4103/0257-7941.107344
2. Prakash, M. V. D., Sampath, S., Amudha, K., Nadeem, A., Lopes, B. S., Durga, B., & Muthupandian, S.,. Materials Technology, 2023 vol. 38(1), p. 2247908, https://doi.org/10.1080/10667857.2023.2247908
3. Adeyemi, J. O., Oriola, A. O., Onwudiwe, D. C., & Oyedeji, A. O., Biomolecules, 2022, vol. 12(5), p. 627. https://doi.org/10.3390/biom12050627
4. Theyyathel, A. M., Nanda, A., SOFI, M. A., & Nayak, B. K., Pak. J. Bot, 2026, vol. 58, p. 4. http://dx.doi.org/10.30848/PJB2026-4(7)
5. Reddy, M., Murthy, K., Srilakshmi, A., Sambasiva Rao, K., & Pullaiah, T., African Journal of Biotechnology, 2015, vol. 14(3), p. 222–247. https://doi.org/10.4314/ajb.v14i3.
6. Ali, S. G., Ansari, M. A., Alzohairy, M. A., Alomary, M. N., AlYahya, S., Jalal, M., Khan, H. M., Asiri, S. M. M., Ahmad, W., Mahdi, A. A., El-Sherbeeny, A. M., & El-Meligy, M. A., Antibiotics, 2020, vol. 9(3), p. 100. https://doi.org/10.3390/antibiotics9030100
7. Al-Rimawi, F., Abu-Lafi, S., Abbadi, J., Alamarneh, A. A. A., Sawahreh, R. A., & Odeh, I., African journal of traditional, complementary, and alternative medicines(AJTCAM), 2017, vol. 14(2), p. 130–141. https://doi.org/10.21010/ajtcam.v14i2.14
8. Abbasi, T., Anuradha, J., & Abbasi, S. A., Nanosci Technol, 2014, vol. 1(3), p. 1-7.
9. Zong, L., Sang, R., Zhang, X., Lim, J. L., Zhao, S., Deng, W., ... & Gu, Z., Nano Letters, 2026, https://doi.org/10.1021/acs.nanolett.5c05084
10. Eker, F., Akdaşçi, E., Duman, H., Bechelany, M., & Karav, S., Nanomaterials, 2024, vol. 14(22), p. 1854. https://doi.org/10.3390/nano14221854
11. Hamza, S. S., Mahdi, R. T., Adil, B. H., Hameed, B. S., & Obaid, A. S., BioNanoScience, 2026, vol. 16(1), p. 26. https://doi.org/10.1007/s12668-025-02158-0
12. Akintelu, S.A., Yao, B. & Folorunso, A.S., Plasmonics, 2021, vol. 16, p. 157–165. https://doi.org/10.1007/s11468-020-01274-9
13. Shaikh JR, Patil M., International journal of chemical studies, 2020, vol. 8 p. 603–608. https://doi.org/10.22271/chemi.2020.v8.i2i.8834

14. Bindhu M, Umadevi M., Materials Letters, 2014, vol. 120, p. 122–125 https://doi.org/10.1016/j.matlet.2014.01.108
15. Fouda, A., Eid, A. M., Guibal, E., Hamza, M. F., Hassan, S. E.-D., Alkhalifah, D. H. M., & El-Hossary, D., Applied Sciences, 2022, vol. 12(24), p. 12879. https://doi.org/10.3390/app122412879
16. Eid, M.M., Characterization of Nanoparticles by FTIR and FTIR-Microscopy. In: Handbook of Consumer Nanoproducts. Springer, Singapore, 2021, https://doi.org/10.1007/978-981-15-6453-6_89-1
17. Anadozie, S. O., Adewale, O. B., Sibuyi, N. R., Fadaka, A. O., Isitua, C. C., Davids, H., & Roux, S., Process Biochemistry, 2023, vol. 128, p. 49-57. https://doi.org/10.1016/j.procbio.2023.02.010
18. Patel, U., Girme, A., Patel, K. et al., JPC-J Planar Chromat., 2021, vol. 34, p. 217–228. https://doi.org/10.1007/s00764-021-00115-7
19. Vignesh A, Selvakumar S, Vasanth K., Phytomedicine plus 2022, vol. 2, p. 100167. https://doi.org/10.1016/j.phyplu.2021.100167
20. Royani, A., Hanafi, M., Julistiono, H., Dinoto, A., Lotulung, P. D. N., & Manaf, A., Trends in Sciences, 2023, vol. 20(1), p. 3884-3884. https://doi.org/10.48048/tis.2023.3884
21. Maheshwaran, L., Nadarajah, L., Senadeera, S. P. N. N., Ranaweera, C. B., Chandana, A. K., & Pathirana, R. N., Asian Plant Research Journal, 2024, vol. 12(5), p. 11-38. https://doi.org/10.9734/aprj/2024/v12i5267
22. Rao, A., Kumari, S., Laura, J. S., & Dhania, G., Journal of Innovation in Psychology, Education and Didactics, 2024, vol. 28(2), p. 621. https://dx.doi.org/10.13005/ojc/390312
23. Mercy Gospel Ajuru, Light Femi Williams, Gospel Ajuru., Journal of Food and Nutrition Sciences, 2017, vol. 5(5), p. 198-205. https://doi.org/10.11648/j.jfns.20170505.16
24. Gurupriya S, Cathrine L, Ramesh J.,Int J Res Appl Sci Eng Technology, 2017,vol. 5,p. 475–479.
25. Roghini R, Vijayalakshmi K., International Journal of Pharmaceutical Sciences and Research, 2018, vol. 9, p. 4859–4864.
26. Praiwala, B., Priyanka, S., Raghu, N., Gopenath, N., Gnanasekaran, A., Karthikeyan, M.,& Basalingappa, K. M., Journal of Biomedical Sciences, 2018, vol. 5(2), p. 10-17.
27. Praveen G, Rajesh G.,Journal of Drug Delivery & Therapeutics, 2018,vol. 8, p. 259–264. https://doi.org/10.22270/jddt.v8i5-s.1967
28. Kaur, G., Prabhakar, P. K., Lal, U. R., & Suttee, A.,International journal of toxicological and pharmacological research, 2016, vol. 8(4), p. 297-305.
29. Kareppa, M.S., Jangme C.M., Patil A.R.,Journal of Neonatal Surgery, 2025, vol. 14.
30. Alhiti, L.S., Hashim, E.H., Abdullah, F.H., Humanities & Natural Sciences Journal 2025, vol. 6, p. 249–265. https://doi.org/https://doi.org/10.53796/hnsj63/12
31. Bharadwaj, K. K., Rabha, B., Pati, S., Sarkar, T., Choudhury, B. K., Barman, A., Bhattacharjya, D., Srivastava, A., Baishya, D., Edinur, H. A., Abdul Kari, Z., & Mohd Noor, N. H., Molecules, 2021, vol. 26(21), p. 6389. https://doi.org/10.3390/molecules26216389
32. Akhtar, S., Zuhair, F., Nawaz, M., & Khan, F. A., RSC advances, 2024, vol. 14(49), p. 36576-36592. https://doi.org/10.1039/D4RA06340F
33. Sadiq, Z., Safiabadi Tali, S. H., Hajimiri, H., Al-Kassawneh, M., & Jahanshahi-Anbuhi, S., Critical Reviews in Analytical Chemistry, 2024, vol. 54(7), p. 2209-2244.https://doi.org/10.1080/10408347.2022.2162331
34. Bhattacharjee, T. T., Castilho, M. L., de Oliveira, I. R., Jesus, V. P. S., Hewitt, K. C., & Raniero, L., Biochimica et Biophysica Acta (BBA)-General Subjects, 2018, vol. 1862(3), p. 495-500. https://doi.org/10.1016/j.bbagen.2017.11.009
35. Oliveira, A. E. F., Pereira, A. C., Resende, M. A. C., & Ferreira, L. F., Analytica, 2023, vol. 4(2), p. 250-263. https://doi.org/10.3390/analytica4020020
36. Kumalasari, M. R., Alfanaar, R., & Andreani, A. S., Talanta Open, 2024, vol. 9, p. 100327. https://doi.org/10.1016/j.talo.2024.100327
37. Gothainayagi, A., Characterization of green synthesized gold nanoparticles from Nigella sativa oil and evaluation of its antibacterial and anticancer activity. Journal of Critical Reviews, 2020.
38. Nagalingam, M., Kalpana, V. N., Devi Rajeswari, V., & Panneerselvam, A Biotechnology Reports, 2018, vol. 19, p. e00268. https://doi.org/10.1016/j.btre.2018.e00268
39. Latha, D., Sampurnam, S., Arulvasu, C., Prabu, P., Govindaraju, K., & Narayanan, V. Materials Today: Proceedings, 2018, vol. 5(2), p. 8968-8972. https://doi.org/10.1016/j.matpr.2017.12.337
40. Modena, M. M., Rühle, B., Burg, T. P., & Wuttke, S., Advanced Materials, 2019, vol. 31(32), p. 1901556. https://doi.org/10.1002/adma.201901556
41. Titus, D., Samuel, E. J. J., & Roopan, S. M. (2019). Nanoparticle characterization techniques. In Green synthesis, characterization and applications of nanoparticles (pp. 303-319). Elsevier. https://doi.org/10.1016/B978-0-08-102579-6.00012-5
42. Fang, X., Szołtysik, R., Tang, J., & Bajkacz, S., Journal of Food Composition and Analysis, 2022, vol. 110, p. 104580. https://doi.org/10.1016/j.jfca.2022.104580
43. Girme, A., Saste, G., Singh, R., Mirgal, A., Ingavale, R., Balasubramaniam, A. K., ... & Hingorani, L., Separation Science Plus, 2022, vol. 5(8), p. 378-392. https://doi.org/10.1002/sscp.202200048
44. Sharma, B., Yadav, A. & Dabur, R., Sci Rep, 2019, vol. 9, p. 14327. https://doi.org/10.1038/s41598-019-50801-0
45. Mittal, R., Patel, A. P., Jhaveri, V. M., Kay, S. I. S., Debs, L. H., Parrish, J. M., … Jayant, R. D., Expert

Opinion on Drug Delivery, 2018, vol. 15(3), p. 301–318. https://doi.org/10.1080/17425247.2018.1420055

46. Li, Y., Wang, H., Si, N., Ren, W., Han, L., Xin, S., Bian, B., Xenobiotica, 2015, vol. 45(4), p. 302–311. https://doi.org/10.3109/00498254.2014.979270
47. Wang, W., Liu, J., Zhao, X., Peng, Y., Wang, N., Lee, D. Y., & Dai, R., Biomedical chromatography, 2017, vol. 31(6), p. e3903. https://doi.org/10.1002/bmc.3903